



π^0 Azimuthal Anisotropy in Au+Au Collisions at $\sqrt{s_{NN}} = 39 - 200$ GeV from PHENIX: Collision Energy and Path-Length Dependence of Jet-Quenching and the Role of Initial Geometry

Xiaoyang Gong^a for the PHENIX Collaboration

^aChemistry Department, Stony Brook University, Stony Brook, NY 11794, USA

Abstract

The azimuthal anisotropy of high p_T particle production in heavy ion collisions is a sensitive probe of the jet quenching mechanism. Recent PHENIX measurements for Au+Au collisions at $\sqrt{s_{NN}} = 200$ GeV show a $\pi^0 v_2$ signal that exceeds the pQCD energy loss calculations up to $p_T \sim 10$ GeV/c, challenging the traditional perturbative picture of the energy loss process. Here, we present an update and details of that measurement, as well as new high p_T measurements at $\sqrt{s_{NN}} = 62$ and 39 GeV. These measurements not only provide an important constraint for understanding the path-length dependence of jet energy loss and the role of initial collision geometry, but also allow a search for the onset of jet quenching as $\sqrt{s_{NN}}$ is varied.

The discovery of the suppression of both high p_T single particle yields [1] and back-to-back jet yields in two particle correlation measurements [2] (“jet-quenching”) is considered one of the most convincing piece of evidence that de-confined matter (or a quark gluon plasma [QGP]) is created in relativistic heavy ion collisions at RHIC. The study of jet quenching has developed into a full-fledged field with precise differential measurements and quantitative theoretical calculations. However, our current understanding of jet quenching faces several challenges: on the one hand, the AdS/CFT approach to describe jet-medium interactions seems to be favored by several measurements (e.g. R_{AA} for non-photonic electrons [3] and high $p_T v_2$ [4]) over the traditional pQCD based treatment; on the other hand, different models which operate inside the pQCD framework, show large differences in their predicted quenching parameters, even though they are embedded into the same evolving medium characterized by 3D hydro and tuned to reproduce central R_{AA} [5]. Precisely measured anisotropy at high p_T , can shed new insights on both challenges.

In 2007, PHENIX accumulated a large dataset of Au+Au Collisions at $\sqrt{s_{NN}} = 200$ GeV with several Reaction Plane (RP) detectors which spanned a broad pseudorapidity (η) range. They included an inner ring (RXNin) ($1.0 < \eta < 1.5$) and an outer ring (RXNout) ($1.5 < \eta < 2.8$) of a newly installed reaction plane detector (RXN), a beam beam counter (BBC) and the muon piston calorimeter (MPC) ($3.1 < \eta < 3.9$). These RP detectors not only provided precise measurements of the Event Plane (EP) but also enabled a systematic examination of non-flow effects, such as a possible jet bias. In 2010, RHIC initiated the energy scan program and PHENIX collected several datasets for Au+Au collisions at $\sqrt{s_{NN}} = 62$ and 39 GeV with significant statistics with the same set of RP detectors as in 2007. The Measurements of $\pi^0 v_2$ from all of these datasets are discussed in the following.

The techniques used for data analysis are adopted from Ref. [4]. Briefly, photons are identified and measured using the electromagnetic calorimeter (EMCal). The invariant mass for photon pairs is sampled over events and a statistical subtraction is implemented to remove the combinatoric background; the shape of the latter is estimated via the widely used event-mixing technique. An integral of the subtracted invariant mass distribution gives the π^0 yield. The emission angle of π^0 relative to the EP ($\Delta\phi$) is folded into $[0, \pi/2]$ (due to the symmetry in the event-

averaged collision geometry; 0 for in-plane and $\pi/2$ for out-plane) and further divided into six angular bins; π^0 yield is measured individually in each of the angular bins. The resulting modulation of “ π^0 yield vs. $\Delta\phi$ ” is Fourier analyzed [6] to obtain the v_2 term. A fit gives the so-called v_2^{raw} and the true corrected v_2 is the quotient v_2^{raw}/σ_{RP} , where σ_{RP} ’s are RP resolution correction factors. These factors characterize the dispersion of the measured EP (Ψ) relative to the “true” RP (Ψ_{RP}) and are defined as $\sigma_{RP} \equiv \langle \cos 2(\Psi - \Psi_{RP}) \rangle$ [6].

The π^0 v_2 results for the three collision energies are shown in the left panel of Fig-1. For both central (0 – 20%) and mid-central (20 – 40%) events the v_2 values for the respective beam energies are quite similar. However, only the 200 GeV data has the statistical significance to probe higher p_T ’s ($> 6.0\text{GeV}$) where jet fragments dominate hadron production. Below 6 GeV v_2 is described by hydrodynamics at low p_T ($< 2.0\text{GeV}$) and recombination at intermediate p_T (2.0 – 6.0GeV); the good agreement of v_2 ’s across collision energies indicates that v_2 is saturated in these two regions. To facilitate the investigation of v_2 saturation, the v_2 vs. $\sqrt{s_{NN}}$ plot is presented on the right panel of Fig-1. At low p_T , our measurements, while showing good agreement with charge hadron results for 200 and 62GeV from [7], add one more point at 39GeV. Combined with v_2 at even lower $\sqrt{s_{NN}}$ at 17 and 3GeV (measured by CERES and E895 respectively), it seems that a transition to saturation is observed. At intermediate p_T , v_2 ’s are saturated down to 39GeV as well.

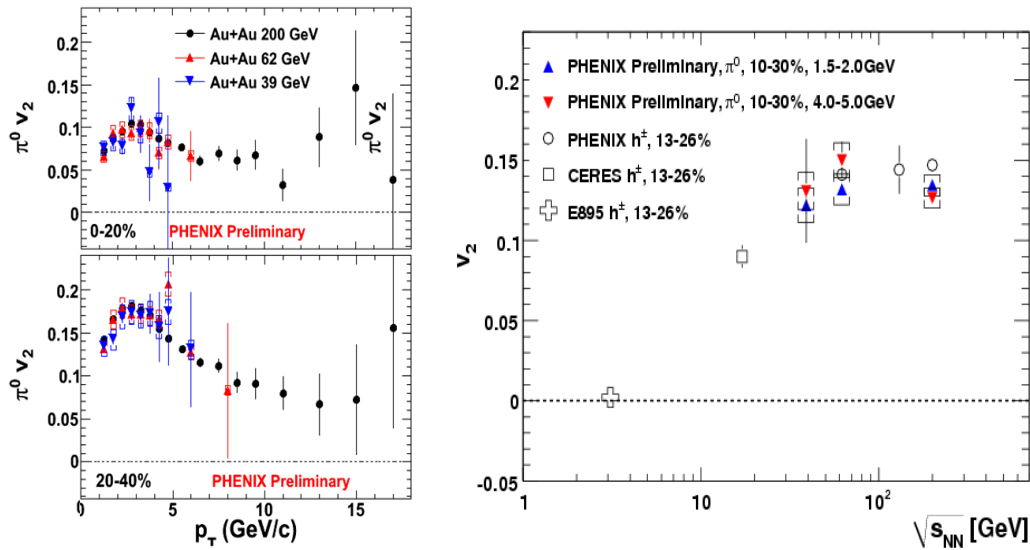


Figure 1: Left panel: π^0 v_2 vs. p_T for 200, 62 and 39GeV for centrality 0 – 20% and 20 – 40%. Right panel: a v_2 energy scan with π^0 and charge hadron (from [7]; all charge hadron data are of p_T 1.5 – 2.0GeV). Statistical errors are indicated by bars and systematic errors by square brackets.

In the following we focus on the high p_T region and discuss results from 200 GeV only. A complementary measurement is v_2 and R_{AA} for the η meson, which is reconstructed from two photons as well and analyzed in the same manner as for the π^0 . The η has a larger mass so its yield can only be extracted for $p_T > 4.0\text{GeV}$ in PHENIX; this is the region where jet-medium interactions play a central role. η v_2 and R_{AA} as a function of p_T are shown in Fig-2 for central (0 – 20%) and mid-central (20 – 60%) collisions; the π^0 results are overlaid to aid a comparison. The measurements show solid agreement within one standard deviation. This observation indicates that mass and quark contents have little effects on high p_T v_2 and R_{AA} , and probably the underlying jet-quenching mechanism as well.

Fig-3 shows π^0 v_2 and R_{AA} vs. N_{part} (number of participants) for $6 \leq p_T \leq 9$ GeV/c. The results from four popular pQCD model calculations are also plotted for comparison. Note that the parameters for these models are tuned to match R_{AA} for the most central collisions. It is clear that while all the models successfully reproduce R_{AA} for a good range of N_{part} ¹, they substantially under-predict v_2 . Moreover, since v_2 and R_{AA} are anti-correlated as indicated by

¹the WHDG model undershoots the data points because it is tuned in the p_T range 5 ~ 18 GeV/c and tends to undershoot the low p_T end.

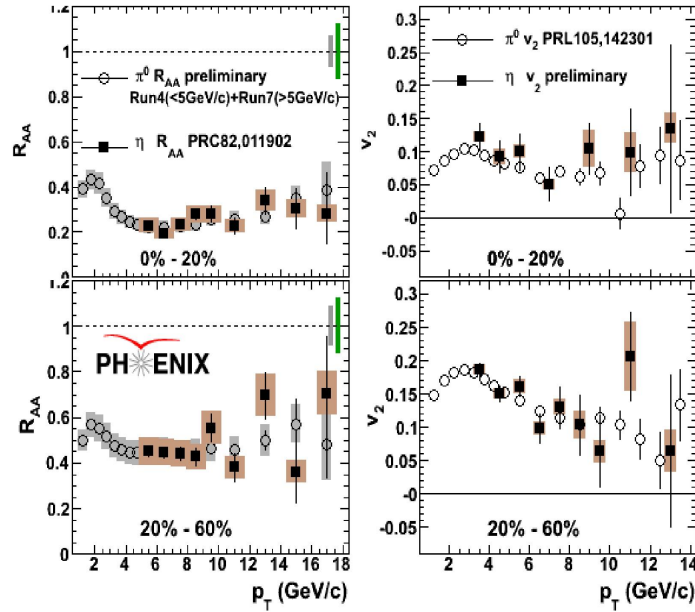


Figure 2: η (black square) R_{AA} (left) and v_2 (right) vs. p_T , overlaid on π^0 results (grey circle) for comparisons. Two centrality ranges are presented: 0 – 20% (top) and 20 – 60% (bottom).

the solid edge on the WHDG band on the figure, the measurements of v_2 and R_{AA} can not be simultaneously described by these models. This discrepancy might be rooted in a combination of different effects. In Ref. [8] different initial collision geometries were considered; instead of the default usage of Glauber Model geometries, the CGC type of geometry as well as its event-by-event fluctuations were taken into account. However, the resulting enhancement of v_2 was not able to account for the whole gap. Subsequently, a model calculation based on AdS/CFT like jet-medium interactions was tested. The idea is that all the models above are based on pQCD; the underestimation of v_2 may suggest that a stronger jet-medium interaction and thus, stronger path-length (L) dependence of jet-quenching is necessary. The AdS/CFT type of path-length dependence is L^3 , stronger than the pQCD counterpart L^2 . This modification is remarkably effective; combined with CGC geometry and event-by-event fluctuation, the reproduced v_2 matches data points well.

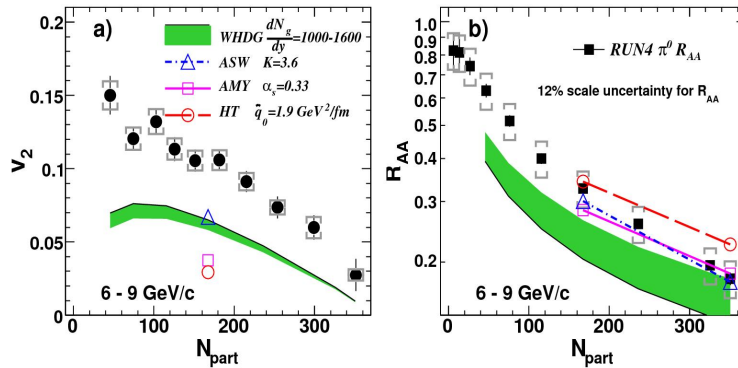


Figure 3: π^0 v_2 and R_{AA} vs. N_{part} . Four pQCD models are plotted for comparison: ASW, AMY and HT from [5]; WHDG from [9]. The upper bound of dN_g/dy in WHDG (1600) is indicated by the solid edge on the band.

To further investigate path-length dependence of jet-quenching, angular dependent R_{AA} is introduced and denoted by $R_{AA}(\Delta\phi)$. It combines the absolute suppression level R_{AA} with path-length variations from in-plane to out-plane. Fig-4 shows high p_T ($7 \sim 8$ GeV/c) π^0 $R_{AA}(\Delta\phi)$ measured for 6 $\Delta\phi$ bins in 6 centrality bins from the most central up to 60%. For each $\Delta\phi$ and centrality bin the path-length integral I_m ($m = 1, 2$) is calculated based on an initial geometry represented by ρ . On the right panel of the figure, where assumptions of an AdS/CFT like jet-medium interaction (I_2) and CGC geometry with event-by-event fluctuation (ρ_{CGC}^{Fluc}) are made, R_{AA} scales remarkably with path-length integrals. This scaling suggests that the inclusive R_{AA} and v_2 for different centralities (or N_{part}) will be automatically and simultaneously described.

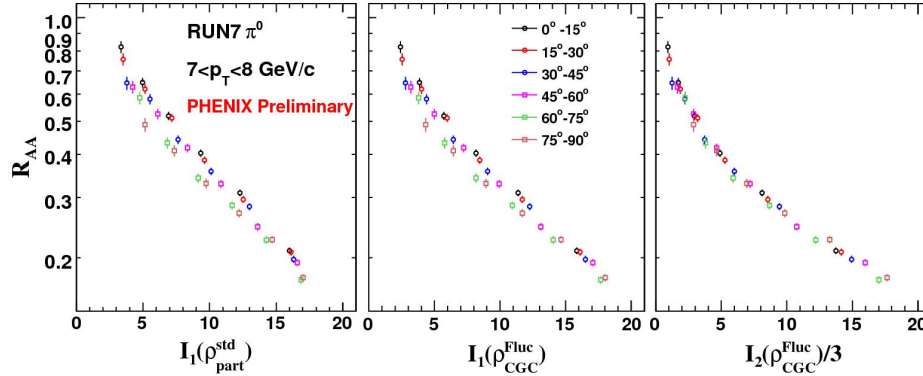


Figure 4: $R_{AA}(\Delta\phi, centrality)$ vs. I_m : $R_{AA}(\Delta\phi, centrality)$ is measured in 6 $\Delta\phi$ bins and 6 centrality ranges; I_m is the path-length integral and $m = 1, 2$ corresponds to pQCD and AdS/CFT like jet-medium interactions respectively. ρ represents initial condition: ρ_{part}^{std} for default Glauber geometry and ρ_{CGC}^{Fluc} for CGC geometry with event-by-event fluctuation.

In summary, π^0 v_2 's for 200, 62 and 39 GeV are measured. In the low and intermediate p_T range, v_2 is saturated across energies. For higher p_T values we found that current pQCD models are challenged to reproduce the π^0 v_2 and R_{AA} simultaneously. However, an AdS/CFT-based calculation that encodes an L^3 path-length dependence with an event-by-event fluctuating CGC geometry is favored by the measurements.

Acknowledgments

This work is supported by the US DOE under contract DE-FG02-87ER40331.A008 and by the NSF under award number PHY-1019387.

References

- [1] K. Adcox et al. (PHENIX Collaboration), Phys. Rev. Lett. **88**, 022301 (2001).
- [2] C. Adler et al. (STAR Collaboration), Phys. Rev. Lett. **90**, 082302 (2003).
- [3] A. Adare et al. (PHENIX), Phys. Rev. Lett. **98**, 172301 (2007), nucl-ex/0611018.
- [4] A. Adare et al. (PHENIX Collaboration), Phys. Rev. Lett. **105**, 142301 (2010).
- [5] S. A. Bass et al., Phys. Rev. C **79**, 024901 (2009).
- [6] A. M. Poskanzer et al., Phys. Rev. C **58**, 1671 (1998).
- [7] S. S. Adler et al. (PHENIX Collaboration), Phys. Rev. Lett. **94**, 232302 (2005).
- [8] J. Jia, Phys. Rev. C **82**, 024902 (2010).
- [9] S. Wicks et al., Nuclear Physics A **784**, 426 (2007), ISSN 0375-9474.



Available online at www.sciencedirect.com



Procedia Computer Science 00 (2019) 1–1

**Procedia Computer
Science**

Abstract

Keywords:

1.

arXiv:1012.1639v1 [nucl-ex] 7 Dec 2010